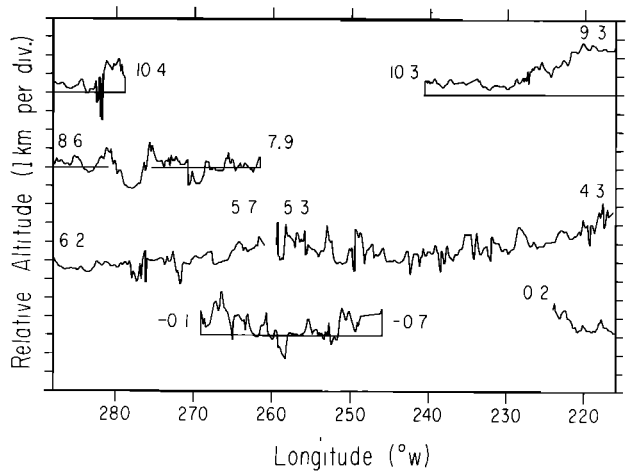

Fig. 2*d*. Altitude profiles for the H-9 quadrangle (216°–288°W longitude). The display format follows that of Figure 2*a* (see caption). This entire quadrangle lies in the unimaged hemisphere.

crater rim heights if the rim crest fills only a small fraction of the area of the radar resolution cell. There may also be a corresponding tendency to underestimate crater floor depths, although the intrinsically high radar cross sections of crater floors should mitigate this effect. Finally, a bias can be introduced if the crater floor is offset to the north or south of the subradar track, in which case the measured depth will include a contribution from the planet's spherical figure. This bias amounts to 0.37 km for a 1° latitude offset, and increases as the square of the offset. The most striking example of this effect is the anomalous 6 km drop seen at 143°W, 1.8°S (Figure 2*b*). This is apparently a signature of the crater Theophanes, which lies 2.5° south of the nominal subradar track. This is an extreme case, however, and in most cases we would expect the upward depth bias due to planet curvature to be about 10% or less. We have elected not to correct for the curvature bias because of (1) the potential errors in subradar latitude associated with uncertainties in the true pole position, and (2) the likelihood that this bias will be offset to some extent by underestimation of the rim height.

In Table 3 are listed the radar-derived depth estimates for 23 craters ranging from 40 to 260 km in diameter. Only craters in the imaged hemisphere of Mercury are included.

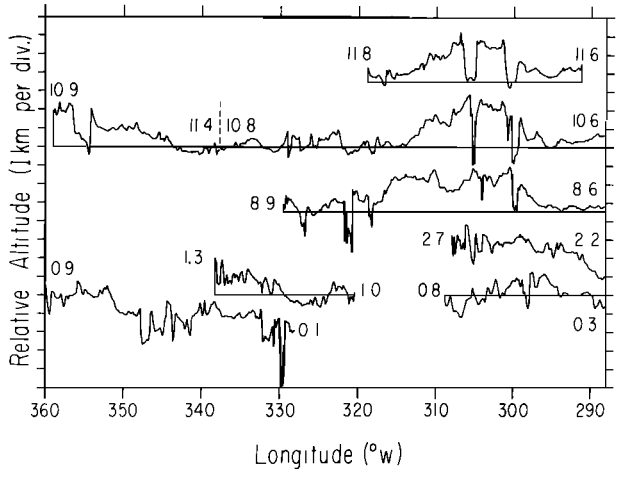

Fig. 2*e*. Altitude profiles for the H-10 quadrangle (288°–360°W longitude). The display format follows that of Figure 2*a* (see caption). This entire quadrangle lies in the unimaged hemisphere.

TABLE 3. Mercury Crater Depth Estimates

Name	Position	Diameter, km	Depth, km	Class
Mozart	190.6°W, 8.0°N	260	2.9	1
Handel	34.0°W, 3.9°N	155	3.1	1
Chaikovskij	50.5°W, 8.0°N	145	2.4	2
Lysippus	133.0°W, 1.3°N	130	1.8	2
Zeami	147.6°W, 2.5°S	123	2.4	1
Rudaki	54.5°W, 3.5°S	115	1.8	2
Thakur	63.8°W, 2.7°S	105	2.3	2
Tyagaraja	148.9°W, 4.3°N	104	4.1	1
Yeats	34.9°W, 9.7°N	100	2.0	1
	82.1°W, 7.3°N	100	1.4	1
	59.9°W, 3.5°S	99	2.5	2
Lu Hsun	24.0°W, 0.1°S	98	3.1	1
Asvaghosa	21.2°W, 10.7°N	86	2.0	1
	129.9°W, 0.1°N	75	2.1	1
	132.8°W, 6.3°N	72	1.8	2
	55.8°W, 3.7°S	65	2.7	1
	121.9°W, 5.4°N	58	1.8	2
	117.8°W, 6.0°N	55	1.8	1
	119.0°W, 0.2°N	51	2.0	2
	132.7°W, 4.0°N	50	2.5	2
	115.7°W, 5.2°N	48	1.8	2
	110.5°W, 5.5°N	41	1.2	2
	113.5°W, 6.5°N	40	1.9	2

Degradational states for these craters were obtained from the geologic maps of the H-6 and H-8 quadrangles [*Schaber and McCauley*, 1980; *De Hon et al.*, 1981] and were estimated for the H-7 quadrangle from Mariner 10 images and the USGS shaded-relief map of the quadrangle. Following the treatment of *Malin and Dzurisin* [1977], we have grouped the craters into "fresh" or class 1 (USGS classes C_3–C_5) and "degraded" or class 2 (USGS classes C_1–C_2) and have plotted their depths as a function of diameter (Figure 3). Included in Figure 3 are the Mariner 10 shadow-derived depth data of *Malin and Dzurisin* [1977]; their power-law relation for fresh Mercurian craters is plotted along with an envelope encompassing their range of values for both fresh and degraded craters. Also shown in Figure 3 is the power-law depth/diameter relation

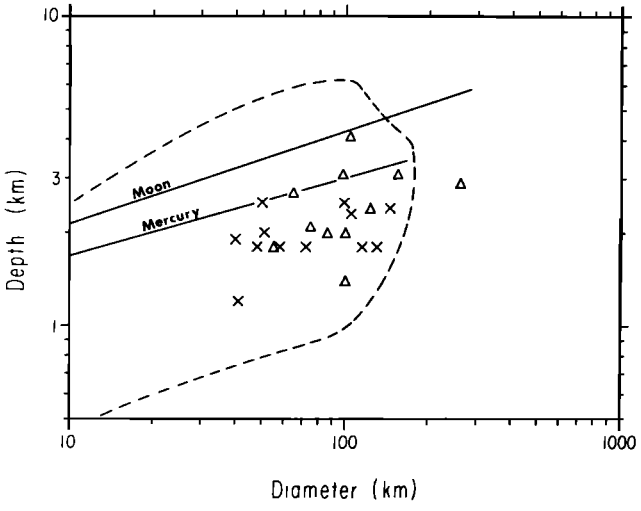

Fig. 3. Depth versus diameter for fresh class 1 (triangles) and degraded class 2 (crosses) Mercurian craters as measured by radar altimetry (Table 3). The dotted line shows the approximate range of shadow-derived depth values for fresh and degraded Mercurian craters [*Malin and Dzurisin*, 1977]. The straight lines are the fitted power-law depth/diameter relations for fresh craters on the moon [*Pike*, 1974] and Mercury [*Malin and Dzurisin*, 1977].